A new methane adsorbent was synthesized from a coordination polymer. This material adsorbs the gas to a remarkable extent and opens up new dimensions for the study of inorganic – organic hybrid adsorbents based on coordination polymers. Find out more on the following pages.

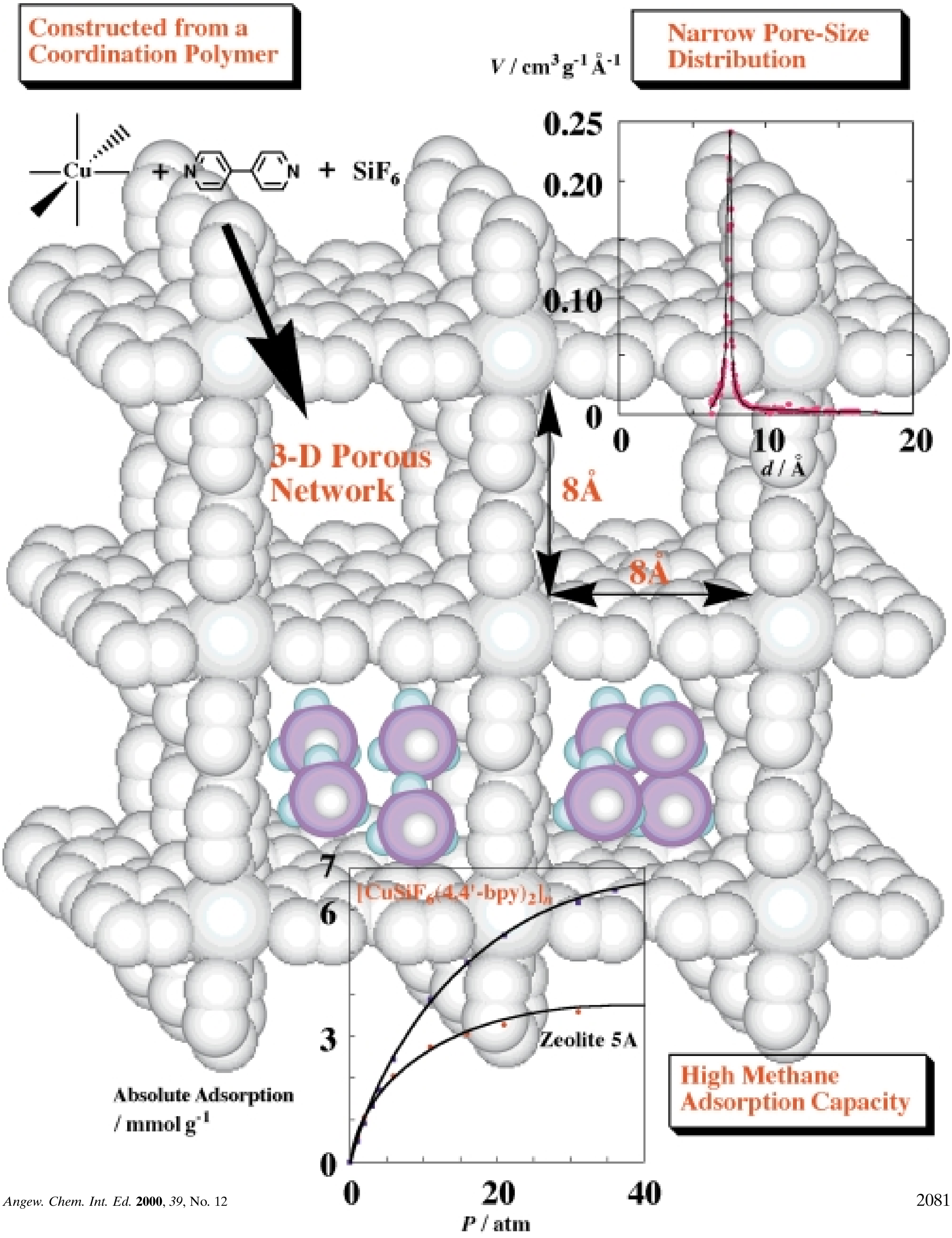

A New, Methane Adsorbent, Porous Coordination Polymer [{$CuSiF_6$(4,4′-bipyridine)$_2$}$_n$]

Shin-ichiro Noro, Susumu Kitagawa,* Mitsuru Kondo, and Kenji Seki

The chemistry of microporous compounds has been studied extensively because of their unique applications, which includes size-selective separation, gas adsorption, heterogeneous catalysis. The creation of porous materials as adsorbents is an attractive research field for the storage and transport of natural gas. So far, porous inorganic materials such as zeolites, aluminum phosphates, and their derivatives have been studied in great detail.[1–3] More recently, coordination polymers constructed from transition metal ions and bridging organic ligands have afforded new types of robust crystals with high degree of porosity.[4–7] Although a large number of these crystals have been hitherto synthesized, still lacking are examples of coordination polymers in which the pores are usefully large and which the coordination framework is sufficiently robust and is maintained over a wide pressure region at ambient temperature. In addition, since nature dislikes a vacuum, the target of a large channels is fraught with difficulties during synthesis, which include 1) the occupation of counteranions in the channels; 2) the need to readily form an interpenetrating network; and that 3) the channel network may be disrupted upon removal of the guest molecules.

Therefore, a rational synthetic strategy is a most significant point for the creation of porous coordination polymers. Generally, when water or other solvents coordinate to metal ions, the resulting network is of low dimensionality and often forms no channels. In this paper, we report a novel 3D coordination polymer, [{[$CuSiF_6$(4,4′-bpy)$_2$]$\cdot 8H_2O$)}$_n$] (**1**; 4,4′-bpy = 4,4′-bipyridine). For this compound, we selected Cu^{II} and SiF_6^{2-} as the building blocks for the construction of a coordination framework with high dimensionality. The Cu^{II} ion (d^9) is liable to undergo Jahn–Teller distortion and results in weakly coordinated bond sites in the axial positions. Consequently, SiF_6^{2-} can coordinate to Cu^{II} more easily than water or other solvents. Since the SiF_6^{2-} anion can link the copper atoms located in each nearest-neighbor square-grid layer, the resulting 3D framework is expected to be robust and free from the occupation of channels by uncoordinated counteranions. We report herein on the successful synthesis of a porous coordination polymer using Cu^{II} and SiF_6^{2-}.

Single crystals were obtained by mixing $Cu(BF_4)_2 \cdot 6H_2O$, $(NH_4)_2SiF_6$, and 4,4′-bpy in a water/ethylene glycol (1:3) solvent. X-ray analysis demonstrates the 3D network is based on a square grid of [{Cu(4,4′-bpy)$_2$}$_n$] and pillars of SiF_6^{2-} ions. Figure 1 shows the coordination of the Cu^{II} ion in the crystal. The pyridine rings of the 4,4′-bpy ligand are disordered over two positions and four (pyridine) nitrogen atoms are coordinated to the Cu^{II} center. Association of two F atoms of the SiF_6 anions provides a (4+2) environment. Bridging the Cu^{II} ions with 4,4′-bpy affords a 2D square grid network. The layers are linked with coordingating SiF_6^{2-} ions to give a 3D structure without interpenetration (Figure 2c). This network yields channels with dimensions of about 8 × 8 Å^2 along the *c* axis and about 6 × 2 Å^2 along the *a* and *b* axes, as shown in Figure 2a and 2b, respectively. The channel is filled with eight crystallized water molecules per Cu^{II} ion. A similar network has been obtained for Zn^{II} the compound [{Zn(4,4′-bpy)$_2$(SiF_6)}$_n$] (**2**)[8] was prepared in dimethyl formamide/dioxane (5:2). It has been previously reported that [{Zn(4,4′-bpy)$_2$(H_2O)$_2$}$_n$(SiF_6)$_n$], which contains interpenetrating 2D [{Zn(4,4′-bpy)$_2$(H_2O)$_2$}$_n$] sheets and no channels, was isolated from an aqueous media containing $ZnSiF_6$ and 4,4′-bpy.[9] The framework in **2** is sensitive to the solvent used. In the case of **1**, the choice of dianion was essential and in the preliminary experiments we observed that a use of GeF_6^{2-} instead of SiF_6^{2-} forms a similar porous 3D network, [{$CuGeF_6$(4,4′-bpy)$_2$}$_n$], under the same reaction conditions.

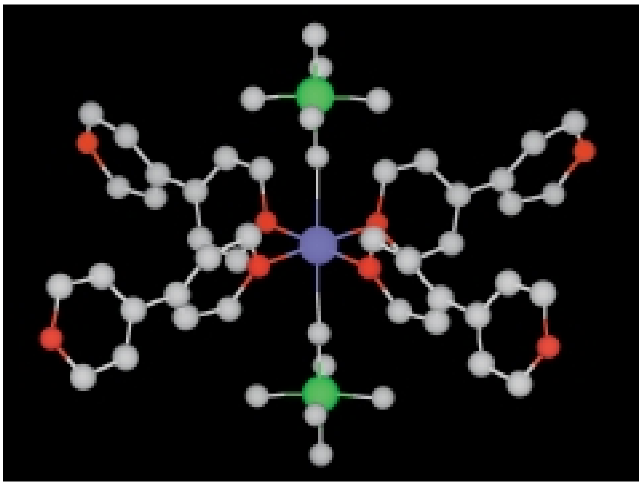

Figure 1. ORTEP representation of the structure around a Cu^{II} center (atomic colors: Cu blue; N red; Si green; C and F gray). Hydrogen atoms and one pyridine ring of the disordered 4,4′-bpy ligand are omitted for clarity. Selected bond lengths [Å]: Cu–F 2.355(5), Cu–N 2.011(5).

The surface area, pore size distribution, and micropore volume of **1** were calculated from argon gas adsorption at 87.3 K measured with a volumetric adsorption apparatus (Micromeritics ASAP 2001M); the data was fitted to the BET equation and to a Horvath–Kawazoe differential pore volume (HK) plot.[10] The HK plot shows only one sharp peak at about 7.8 Å (Figure 2d) to reveal that this material does have a square pore (8 × 8 Å^2) and agrees quantitatively

---

[*] Prof. Dr. S. Kitagawa, Dr. M. Kondo
Department of Synthetic Chemistry and Biological Chemistry
Graduate School of Engineering
Kyoto University
Yoshida, Sakyo-ku, Kyoto 606-8501 (Japan)
Fax: (+81) 75-753-4979
E-mail: kitagawa@sbchem.kyoto-u.ac.jp
S.-i. Noro
Department of Chemistry
Graduate School of Science
Tokyo Metropolitan University
Minami-ohsawa Hachioji-shi, Tokyo 192-0397 (Japan)
K. Seki
Energy Conversion and Storage Technology Applied Research Center
Research and Development Department
Osaka Gas Company, Ltd.
Torishima, Konohana-ku, Osaka 554-0051 (Japan)

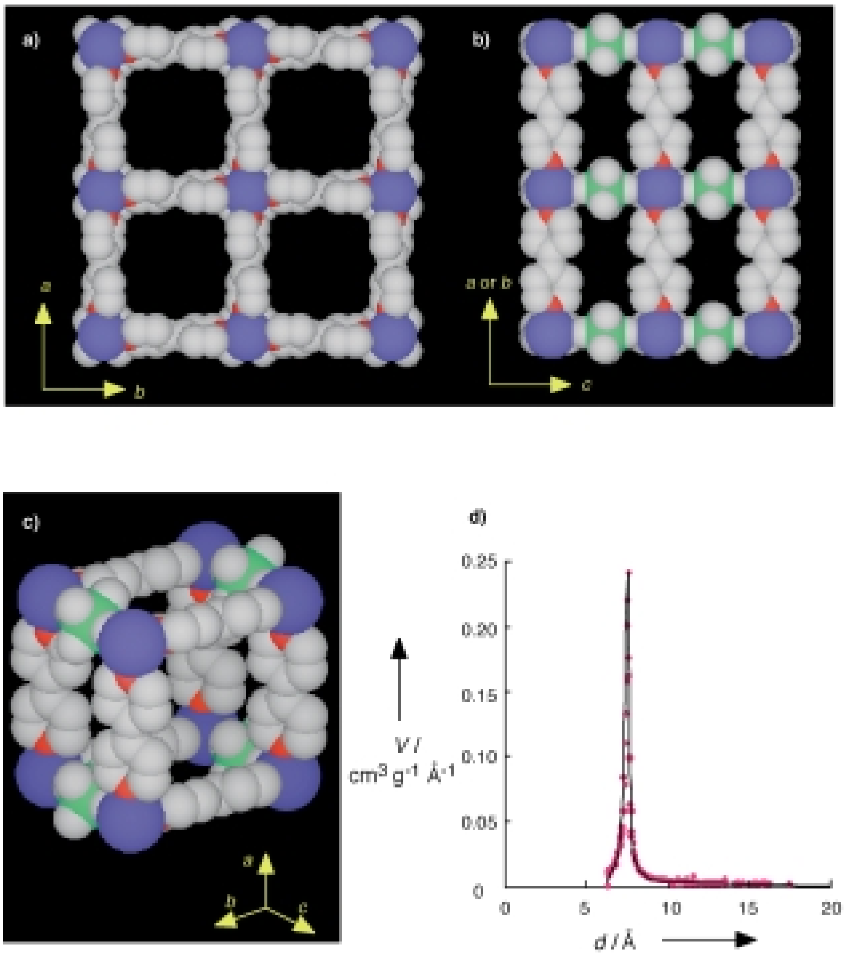

Figure 2. a) Space filling model of the channel structures along the *c* axis. b) Along the *a* or *b* axes. c) The 3D network. Atomic colors are as per Figure 1. The hydrogen atoms, one pyridine ring of the disordered 4,4′-bpy ligand, and crystallized water molecules are omitted for clarity. The pore size given in the text was estimated from this Figure when all the hydrogen atoms are added to the 4,4′-bpy molecules in a space-filling model. d) Horvath–Kawazoe differential pore volume plot. Only one sharp peak at approximately 7.8 Å was observed, which indicates that the size of microporous channels are regular.

with the result of the X-ray analysis. The argon molecules cannot pass the rectangular pore (6×2 Å^2) because of the larger diameter of argon. The micropore volume and specific surface area, on the basis of argon adsorption, are calculated to be 0.56 mL g^{-1} and 1337 m^2 g^{-1}, respectively.

The stability of this network was studied by X-ray powder diffraction (XRPD) and thermal gravimetric (TG) analysis. Figure 3 shows the XRPD patterns at 373 K under high vacuum (approximately 0.1 mm Hg) with a simulated pattern based of the single-crystal data without crystallized water molecules. The TG analysis reveals that the crystallized solvent molecules are absent under the measurement conditions.[11] The good agreement between the peaks in both diagrams demonstrates that the porous network is retained in this phase and indicates that the network is retained in the absence of any guest molecules in the channels.

Methane adsorption experiments were also carried out on **1** and on zeolite 5A, which has the highest known methane adsorption capacity.[12–14] Figure 4 shows the isotherms for methane adsorption in the pressure range 0–36 atm at 298 K. Desorption/readsorption experiments for **1** trace the same isotherm, which indicates that the channel structures are retained throughout this process. At 36 atm, the density of methane adsorbed in the micropores of **1** is 0.21 g mL^{-1}. The density of the compressed methane at 300 K and 280 atm is almost the same as that in **1** at 298 K and 36 atm (= 0.16 g mL^{-1}), indicative of a concentration effect from strong micropore filling in the cavities. The high pressure adsorption of supercritical methane in micropores has been studied with the following extended Dubinin–Radushkevich (DR) equation.[15]

$$\left[\ln\left(\frac{W_\mathrm{L}}{W}\right)\right]^{1/2} = \left(\frac{RT}{\beta E_0}\right)(\ln P_{0q} - \ln P) \qquad (1)$$

Here, the parameters W, βE_0, and P_{0q} are the degree of adsorption at a pressure P, the adsorption energy, and the saturated vapor pressure of the quasi-vaporized supercritical methane, respectively. The large inherent micropore capacity, W_L, of 10.0 mmol g^{-1} is obtained from the Langmuir plot. This isotherm matches the DR equation well. The methane adsorption quantity at high pressure (about 6.5 mmol g^{-1} at 36 atm) is much larger than that of zeolite 5A (about 3.7 mmol g^{-1} at 36 atm). The obtained parameters are $\beta E_0 = 8$ kJ mol^{-1} and $P_{0q} = 284$ atm. In conclusion, this material

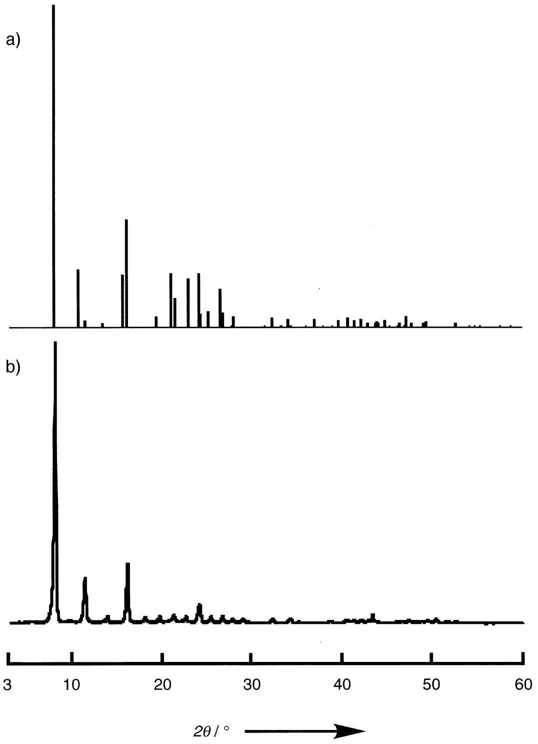

Figure 3. a) Simulated XRPD pattern upon removal of the water molecules from the single crystal and b) the observed pattern under reduced pressure at 373 K.

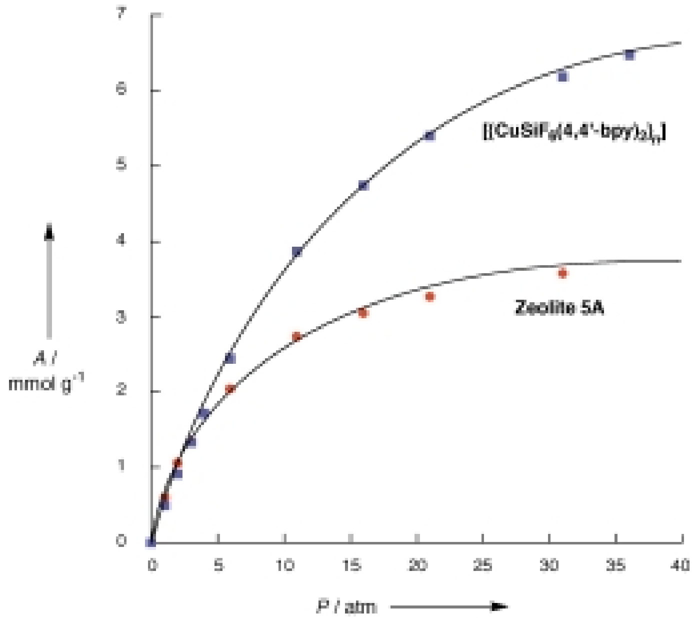

Figure 4. Methane adsorption isotherms at 298 K over a pressure range 0–36 atm (A = absolute adsorption).

has the high adsorption ability and opens up a new dimension for the study of adsorbents of inorganic–organic hybrid materials based on coordination polymers.

Experimental Section

Crystals of **1** suitable for single crystal X-ray analysis were prepared by diffusing an aqueous ethylene glycol solution containing a mixture of $Cu(BF_4)_2 \cdot 6H_2O$ (1.00 mmol) and $(NH_4)_2SiF_6$ (1.00 mmol) into an ethylene glycol solution of 4,4'-bpy (2.00 mmol) using a straight-type glass tube at room temperature. After one week, purple block-shaped crystals had precipitated. Four water molecules per unit cell evaporated in air to give a partly dehydrated compound (yield: 88%). Elemental anal. calcd for $[\{[CuSiF_6(4,4'\text{-bpy})_2] \cdot 4H_2O\}_n]$: C 40.71, H 4.10, N 9.50; found: C 40.81, H 3.50, N 9.27. IR (KBr pellet): $\tilde{\nu} = 3412$ (br), 3098 (w), 3045 (w), 1610 (m), 1535 (w), 1493 (w), 1412 (w), 1221 (w), 1078 (w), 995 (w), 812 (s), 742 (s), 644 (m), 482 cm^{-1} (s).

For the X-ray diffraction, a crystal was mounted on a glass fiber coated with epoxy resin. Measurements were made on a Rigaku Mercury charge-coupled device (CCD) system with graphite monochromated $Mo_{K\alpha}$ radiation. Crystal data: $C_{20}H_{32}CuF_6N_4O_8Si$, $M = 662.12$, tetragonal, space group $P4/mmm$ (No. 123), $a = 11.108(1)$, $c = 8.1107(9)$ Å, $V = 1000.8(1)$ Å^3, $Z = 1$, $\rho_{calcd} = 1.098$ g cm^{-3}, $\lambda(Mo_{K\alpha}) = 0.71069$ Å, $F(000) = 341.00$, $\mu(Mo_{K\alpha}) = 6.38$ cm^{-1}, $T = 233$ K, $2\theta_{max} = 54.9°$, 7187 reflections measured, 937 observed ($I > 2\sigma(I)$), 50 parameters; $R = 0.056$, $R_w = 0.050$. Crystallographic data (excluding structure factors) for the structures reported in this paper have been deposited with the Cambridge Crystallographic Data Centre as supplementary publication no. CCDC-142080. Copies of the data can be obtained free of charge on application to CCDC, 12 Union Road, Cambridge CB21EZ, UK (fax: (+44)1223-336-033; e-mail: deposit@ccdc.cam.ac.uk).

The adsorption isotherms of methane gas on the sample were measured according to the reported procedure.[12, 13] The apparatus was equipped with a Cahn R-100 electrobalance contained within a SUS steel pressure chamber connected with two separate lines for evacuation and adsorbate gas pressurization. After the sample was placed in the apparatus, the solvated molecules in the channels were removed under reduced pressure at 298 K. The removal process was monitored by the reduction in weight. The methane was admitted into the adsorption chamber and then the change in weight of the sample was monitored. The entire adsorption isotherms at 298 K were determined by increasing the adsorbate gas pressure to a maximum of 36 atm. All changes in weight were corrected for buoyancy.

Zeolite 5A was purchased from Bayer. The adsorption isotherms of methane gas were measured with the same method as for the sample. The reported methane adsorption of zeolite 5A by Mentasty et al.[14] (2.9 mmol g^{-1} at 36 atm) was smaller than our result (3.7 mmol g^{-1} at 36 atm). Therefore, we used the higher methane adsorption quantity as comparison data with **1**.

Received: December 21, 1999 [Z14439]

---

[1] A. Corma, *Chem. Rev.* **1997**, *97*, 2373–2419.
[2] G. A. Ozin, A. Kuperman, A. Stein, *Angew. Chem.* **1989**, *101*, 373–390; *Angew. Chem. Int. Ed. Engl.* **1989**, *28*, 359–376.
[3] W. Hölderich, M. Hesse, F. Naumann, *Angew. Chem.* **1988**, *100*, 232–251; *Angew. Chem. Int. Ed. Engl.* **1988**, *27*, 226–246.
[4] S. S.-Y. Chui, S. M.-F. Lo, J. P. H. Charmant, A. G. Orpen, I. D. Williams, *Science* **1999**, *283*, 1148–1150.
[5] H. Li, M. Eddaoudi, M. O'Keeffe, O. M. Yaghi, *Nature* **1999**, *402*, 276–279.
[6] H. Li, M. Eddaoudi, T. L. Groy, O. M. Yaghi, *J. Am. Chem. Soc.* **1998**, *120*, 8571–8572.
[7] M. Kondo, T. Okubo, A. Asami, S. Noro, T. Yoshitomi, S. Kitagawa, T. Ishii, H. Matsuzaka, K. Seki, *Angew. Chem.* **1999**, *111*, 190–193; *Angew. Chem. Int. Ed.* **1999**, *38*, 140–143.
[8] S. Subramanian, M. J. Zaworotko, *Angew. Chem.* **1995**, *107*, 2295–2297; *Angew. Chem. Int. Ed. Engl.* **1995**, *34*, 2127–2129.
[9] R. W. Gable, B. F. Hoskins, R. Robson, *J. Chem. Soc. Chem. Commun.* **1990**, 1667–1668.
[10] G. Horvath, K. Kawazoe, *J. Chem. Eng. Jpn.* **1983**, *16*, 470–475.
[11] The TG curve shows the release of crystallized water molecules to 373 K, which is followed by decomposition of the framework at 423 K.
[12] S.-Y. Zhang, O. Talu, D. T. Hayhurst, *J. Phys. Chem.* **1991**, *95*, 1722–1726.
[13] J. L. Zuech, A. L. Hines, E. D. Sloan, *Ind. Eng. Chem. Process Des. Dev.* **1983**, *22*, 172–174.
[14] L. Mentasty, A. M. Woestyn, G. Zgrablich, *Adsorpt. Sci. Technol.* **1994**, *11*, 123–133.
[15] K. Kaneko, K. Murata, K. Shimizu, S. Camara, T. Suzuki, *Langmuir* **1993**, *9*, 1165–1167.